The Company of Biologists

RESEARCH ARTICLE

Distinct regulation of *Snail* in two muscle lineages of the ascidian embryo achieves temporal coordination of muscle development

Miki Tokuoka, Kenji Kobayashi and Yutaka Satou*

ABSTRACT

The transcriptional repressor Snail is required for proper differentiation of the tail muscle of ascidian tadpole larvae. Two muscle lineages (B5.1 and B6.4) contribute to the anterior tail muscle cells, and are consecutively separated from a transcriptionally quiescent germ cell lineage at the 16- and 32-cell stages. Concomitantly, cells of these lineages begin to express *Tbx6.b* (*Tbx6-r.b*) at the 16- and 32-cell stages, respectively. Meanwhile, *Snail* expression begins in these two lineages simultaneously at the 32-cell stage. Here, we show that *Snail* expression is regulated differently between these two lineages. In the B5.1 lineage, *Snail* was activated through *Tbx6.b*, which is activated by maternal factors, including Zic-r.a. In the B6.4 lineage, the MAPK pathway was cell-autonomously activated by a constitutively active form of Raf, enabling Zic-r.a to activate *Snail* independently of *Tbx6.b*. As a result, *Snail* begins to be expressed at the 32-cell stage simultaneously in these two lineages. Such shortcuts might be required for coordinating developmental programs in embryos in which cells become separated progressively from stem cells, including germline cells.

KEY WORDS: Ascidian, *Ciona*, *Snail*, Germline, Raf

INTRODUCTION

Transcription is repressed in cells with a germ cell fate in many animal embryos, and somatic lineages are progressively separated from the germ lineage in some animals, including nematodes and ascidians (Kumano et al., 2011; Robert et al., 2015; Shirae-Kurabayashi et al., 2011; Strome and Lehmann, 2007) (Fig. 1). In the ascidian *Ciona intestinalis* (type A, also called *Ciona robusta*), which is an invertebrate chordate, germ cells are derived from the most-posterior cells of early embryos. Transcription in this lineage is repressed by Pem-1, and *Pem-1* mRNA is localized at the posterior pole containing the centrosome-attracting body (Hibino et al., 1998; Kumano et al., 2011; Shirae-Kurabayashi et al., 2011; Yoshida et al., 1996). At the 8-cell stage, the vegetal posterior cell pair, known as B4.1, has the potential to give rise to endoderm, mesenchyme, notochord, muscle, and germ cells. At the 16-cell stage, the posterior daughter cells (B5.2) of B4.1 retain the developmental fates of muscle, mesenchyme, and germ cells, and transcription is repressed by Pem-1 in these cells. In the anterior somatic daughter cells (B5.1) of B4.1, several regulatory genes, including *Tbx6.b* (*Tbx6-r.b*), begin to be expressed zygotically. At the 32-cell stage, the posterior daughter cells (B6.3) of B5.2 again

Department of Zoology, Graduate School of Science, Kyoto University Sakyo, Kyoto, 606-8502, Japan.

*Author for correspondence (yutaka@ascidian.zool.kyoto-u.ac.jp)

Y.S., 0000-0001-5193-0708

retain the developmental fates of muscle, mesenchyme, and germ cells, and transcription is repressed, whereas several regulatory genes begin to be expressed zygotically in the anterior somatic daughter cells (B6.4). Thus, at each cell division, the zygotic genetic program is initiated in the sister cells of those cells with a germ cell fate. Although both B5.1 and B6.4 cells contribute to muscle and mesenchyme tissue development, the zygotic genetic programs that specify these fates do not begin simultaneously.

Snail (Snai), which suppresses *Brachyury* encoding a notochord-specific transcriptional activator in muscle cells (Fujiwara et al., 1998; Kobayashi et al., 2003), begins to be expressed at the 32-cell stage in the B5.1 and B6.4 lineages simultaneously (Erives et al., 1998). *Snail* expression begins one stage later than the initiation of the zygotic program in the B5.1 lineage, whereas *Snail* expression begins immediately after the initiation of the zygotic program in the B6.4 lineage. However, it is not clear whether *Snail* expression is regulated by either a common mechanism or different mechanisms in these two lineages.

The maternal factor, Zic-r.a (Macho-1), is required for *Snail* expression in both the B5.1 and B6.4 lineages (Kobayashi et al., 2003; Yagi et al., 2004). *Zic-r.a* mRNA is localized at the posterior pole, similar to *Pem-1* mRNA (Nishida and Sawada, 2001; Satou et al., 2002). *Snail* is regulated under the control of *Tbx6.b* at the gastrula stage (Imai et al., 2006), and *Tbx6.b* is activated by Zic-r.a at the 16-cell stage (Oda-Ishii et al., 2016; Yagi et al., 2004). Therefore, it is likely that Zic-r.a regulates *Snail* indirectly through *Tbx6.b* in the B5.1 lineage. However, in B6.4 cells, *Snail* and *Tbx6.b* begin to be expressed simultaneously at the 32-cell stage and, therefore, it is unlikely that *Snail* expression is regulated by Tbx6.b in this lineage. Hence, *Snail* expression might be regulated differently between the B5.1 and the B6.4 lineages. This suggests that different mechanisms are required for coordinating developmental programs in embryos in which somatic cells become separated progressively from cells with a germ line fate.

In the present study, we demonstrated that *Snail* is regulated differently between these two somatic lineages, which are separated from the germ lineage at the 16-cell and 32-cell stages, respectively. We also provide evidence that *Snail* is under the control of the mitogen-activated protein kinase (MAPK) pathway activated cell-autonomously by a constitutively active form of Raf.

RESULTS

Snail is required for the proper differentiation of muscle cells

Although Snail is known to repress *Brachyury*, which is a key gene for notochord specification, in muscle cells (Fujiwara et al., 1998), no ectopic *Brachyury* expression has been detected in muscle cells of *Snail* morphant embryos [embryos developed from eggs injected with an antisense morpholino oligonucleotide (MO) against *Snail*] (Imai et al., 2006). This implies that Snail is not the only repressor of *Brachyury* in the muscle lineage, as previously suggested (Fujiwara et al., 1998), and that *Snail* has additional functions in this lineage.
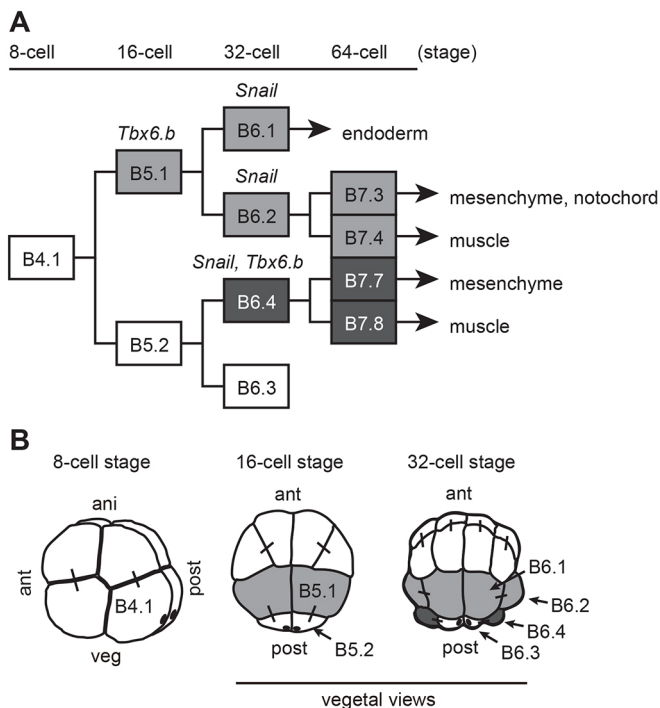
DEVELOPMENT

1

Fig. 1. *Snail* is expressed in the posterior vegetal cells except the most posterior cells at the 32-cell stage. (A) The cell lineage of posterior vegetal blastomeres of bilaterally symmetrical *Ciona* embryos. Cells with a germline fate with repressed transcription are enclosed by white boxes. The B5.1 and B6.4 lineages are marked by light gray and dark gray boxes, respectively. The initiation of zygotic *Snail* and *Tbx6.b* expression is indicated above the boxes. (B) Eight-cell (lateral view), 16-cell (vegetal view) and 32-cell embryos (vegetal view). B5.1 lineage and the B6.4 lineage cells are filled with light gray and dark gray, respectively. Sister cells are connected by short lines. Posterior poles, in which *Zic-r.a* and *Pem-1* are localized, are shown as black ovals.

On the basis of this, we performed an RNA-sequencing (RNA-seq) experiment to understand the function of *Snail*. Given that *Snail* is expressed not only in the muscle lineage, but also in the neural lineage, we used partial embryos to examine *Snail* function in the muscle lineage. We isolated a pair of vegetal posterior cells (B4.1) at the 8-cell stage (Fig. 2A), because most muscle cells derive from this cell pair, and because such partial embryos develop muscle cells (Deno et al., 1984). We prepared partial embryos from unperturbed and *Snail* morphant embryos for RNA-seq. Based on biological duplicates, we found that 118 genes were expressed differentially between these two types of partial embryo (*P*<0.01 and >2-fold-change; 54 and 64 genes were up- and downregulated in *Snail* morphant-derived partial embryos, respectively).

Among these differentially expressed genes, the expression patterns of 16 of the upregulated genes and 27 of the downregulated genes have been revealed at the early tailbud stage (Imai et al., 2004; Miwata et al., 2006; Satou et al., 2001b) (Table S1). Fourteen of the 16 upregulated genes were expressed in the ectoderm (epidermis and/or nervous system), and 22 of the 27 downregulated genes were expressed in muscle (Fig. 2B). One of the upregulated genes, *Myt1*, which is expressed in the nervous system of unperturbed normal tailbud embryos (Fig. 2C), was expressed ectopically in the muscle cells of *Snail* morphants (*n*=24, 100%; Fig. 2D). The downregulation of *Mrf*, which encodes the sole ortholog of vertebrate myogenic regulatory factors and is one of the genes that was downregulated in the RNA-seq experiment, was confirmed by reverse-transcription followed by quantitative PCR (RT-qPCR)

(Fig. 2E). Consistent with the RNA-seq results, the expression of these genes was reduced rather than completely lost. Thus, *Snail* appears to contribute to the suppression of ectodermal genes and the activation of muscle genes in muscle cells.

Two regulatory mechanisms for *Snail* expression in early embryos

To understand how *Snail* is activated in the B5.1 and B6.4 lineages, we first confirmed that *Snail* expression is under the control of Zic-r.a at the 32-cell stage. As previously reported (Yagi et al., 2004), *Snail* expression was lost in *Zic-r.a* morphants (Fig. S1). Given that *Tbx6.b* is required for *Snail* expression at the gastrula stage (Imai et al., 2006), we used *in situ* hybridization to examine whether *Tbx6.b* is required for *Snail* expression at the 32-cell stage. In *Tbx6.b* morphants, whereas *Snail* expression was diminished in the B5.1 lineage (B6.1 and B6.2), it was observed in the B6.4 lineage (Fig. 3). Thus, the regulatory mechanism for *Snail* expression differs between the anterior B5.1 and posterior B6.4 lineages. In the B5.1 lineage, *Snail* expression was regulated under the control of Zic-r.a and Tbx6.b. In the B6.4 lineage, *Snail* expression was not regulated by Tbx6.b.

The MAPK pathway is activated differently in the posterior B-line cells

In contrast to cells of the B5.1 lineage, B6.4 cells begin to express *Snail* immediately after release from transcriptional repression in cells with a germ cell fate. Therefore, it is unlikely that zygotically expressed transcription factors would regulate *Snail* in B6.4. However, we could not rule out the possibility that signaling molecules secreted from surrounding cells regulate *Snail* expression. Given that *Fgf9/16/20* begins to be zygotically expressed in vegetal cells, except B5.2 cells, of 16-cell embryos (Bertrand et al., 2003; Imai et al., 2002a) and activates genes encoding transcription factors and signaling molecules in 32-cell embryos (Bertrand et al., 2003; Hudson et al., 2016; Ikeda et al., 2013; Ikeda and Satou, 2017; Imai et al., 2002b), we next examined *Snail* expression in *Fgf9/16/20* morphants and embryos treated with U0126, which is a specific inhibitor of the MAP kinase kinase, MEK. *Snail* expression did not change in most of the *Fgf9/16/20* morphants (81%; Fig. 4A), although it was weak in B6.4 cells of the remaining embryos (19%). Meanwhile, *Snail* expression in B6.4 cells, but not in the B5.1 lineages (B6.1 and B6.2), was diminished in most of the embryos treated with U0126 (95%; Fig. 4B). This suggested that activation of the MAPK pathway is required for activating *Snail* in B6.4, and that Fgf9/16/20 signaling is not necessarily required for activating the MAPK pathway in the posterior lineage.

Immunostaining with antibodies specifically recognizing doubly phosphorylated ERK (dpERK) showed that this MAPK is activated in all vegetal cells at the 32-cell stage (Fig. 4C), as well as in the neural lineages in the animal hemisphere (Haupaix et al., 2013; Ohta and Satou, 2013; Picco et al., 2007). In *Fgf9/16/20* morphants, dpERK signals were lost from all cells except two pairs of the posterior lineage (B6.3 and B6.4), in which weak signals were detected (Fig. 4D). Similarly, in embryos injected with synthetic mRNA for a dominant negative form of the Fgf receptor (dnFGFR) (Davidson et al., 2006; Hudson et al., 2007), dpERK signals were lost from all cells except two pairs of the posterior lineage (Fig. 4E). In embryos treated with U0126, dpERK signals were completely lost from all cells, including the posterior lineage cells (Fig. 4F). Quantification of the dpERK signal intensities in nuclei showed that the intensity in B6.4 was reduced to ∼25% in *Fgf9/16/20* morphants and embryos injected with dnFGFR mRNA and to almost 0% in U0126-treated embryos compared with control embryos (Fig. 4G).
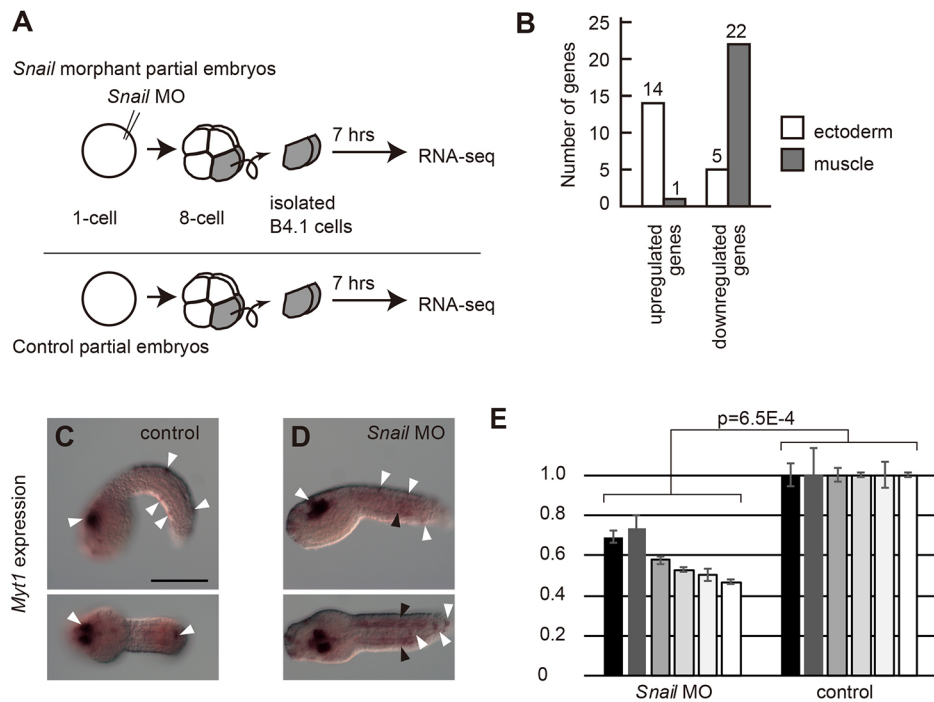
DEVELOPMENT

Fig. 2. RNA-seq identified *Snail* downstream genes. (A) The experimental design. The posterior vegetal cells (B4.1) of 8-cell embryos were isolated with a fine glass needle and incubated for an additional 7 h. Gene expression patterns were compared between embryos derived from unperturbed eggs and those derived from eggs injected with the *Snail* MO. (B) The graph shows the number of up- and downregulated genes expressed in ectodermal cells and muscle cells. (C,D) *Myt1* expression at the tailbud stage of (C) an unperturbed control embryo and (D) a *Snail* morphant embryo (*n*=24). *Myt1* is normally expressed in the nervous system (white arrowheads). In (D), ectopic expression in muscle cells is evident (black arrowheads). (E) Quantification of *Mrf* mRNA, which is expressed specifically in muscle cells, in control and *Snail* morphant embryos at the tailbud stage. Results for six independent experiments are shown by bars of different colors. *Pou2* was used as an internal control for normalization, and the *y*-axis represents normalized relative expression compared with unperturbed embryos. Differences in relative expression were analyzed by paired *t*-tests. Error bars indicate standard errors between technical duplicates. Scale bar: 100 µm.

As well as the nuclear signal, dpERK signals were also detected around the posterior pole, where posterior-end-mark mRNAs, including *Zic-r.a* and *Pem-1*, are localized; these signals were lost in embryos treated with U0126, but not in embryos injected with the *Fgf9/16/20* MO or dnFGFR mRNA (Fig. 4C-F). Thus, the MAPK pathway is also activated around the posterior pole.

The MAPK pathway can be activated cell-autonomously in the B6.4 lineage

The above observation implied that the MAPK pathway was activated cell-autonomously in B6.4 cells. To confirm this hypothesis, using a glass needle, we consecutively isolated posterior blastomeres at the 8- and 16-cell stages (Fig. 5A). At the 8-cell stage, we isolated one of the posterior vegetal blastomeres (B4.1). At this stage, dpERK signals were hardly detected (Fig. 5B). The isolated blastomere divided unequally into a large blastomere and a small blastomere at the time when control embryos become 16-cell embryos. These blastomeres were assumed to correspond to B5.1 and B5.2. Immediately after this division, we again isolated these two cells, and incubated the smaller one, which we assumed to correspond to B5.2. With these manipulations, isolated blastomeres were sequestered from cells with zygotic gene expression, which included cells expressing *Fgf9/16/20*; note that no zygotic transcription has been observed before the 8-cell stage in this animal. When control embryos became 32-cell embryos and the isolated blastomere divided into two cells, which we assumed corresponded to B6.3 and B6.4, we fixed the partial embryos and examined MAPK pathway activity and the expression of *Snail*.

In the experimental embryos, dpERK signals were observed (Fig. 5C), indicating that the MAPK pathway was activated cell-autonomously in this lineage. By contrast, a dpERK signal was rarely observed and was significantly lower in morphant embryos of *Raf*, which encodes a MAP kinase kinase kinase (MAP3K) (Fig. 5D,E). This was also confirmed with another MO targeting a different region of *Raf* mRNA (Fig. 5E). This observation indicated that the cell-autonomous activation of the MAPK pathway began with Raf or its upstream regulator.

Consistently, *Snail* was expressed in one cell of this cell pair derived from uninjected control embryos in all cases (*n*=7) (Fig. 5F), and no clear signal for *Snail* expression was detected in
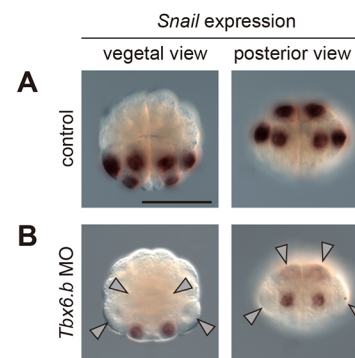

Fig. 3. *Tbx6.b* regulates *Snail* expression only in the B5.1 lineage. *Snail* expression in (A) control and (B) *Tbx6.b* morphant embryos at the 32-cell stage. *Snail* expression was lost in the B5.1 lineage (B6.1 and B6.2; arrowheads), but not in B6.4 of 90% of *Tbx6.b* morphants (*n*=22). Scale bar: 100 µm.
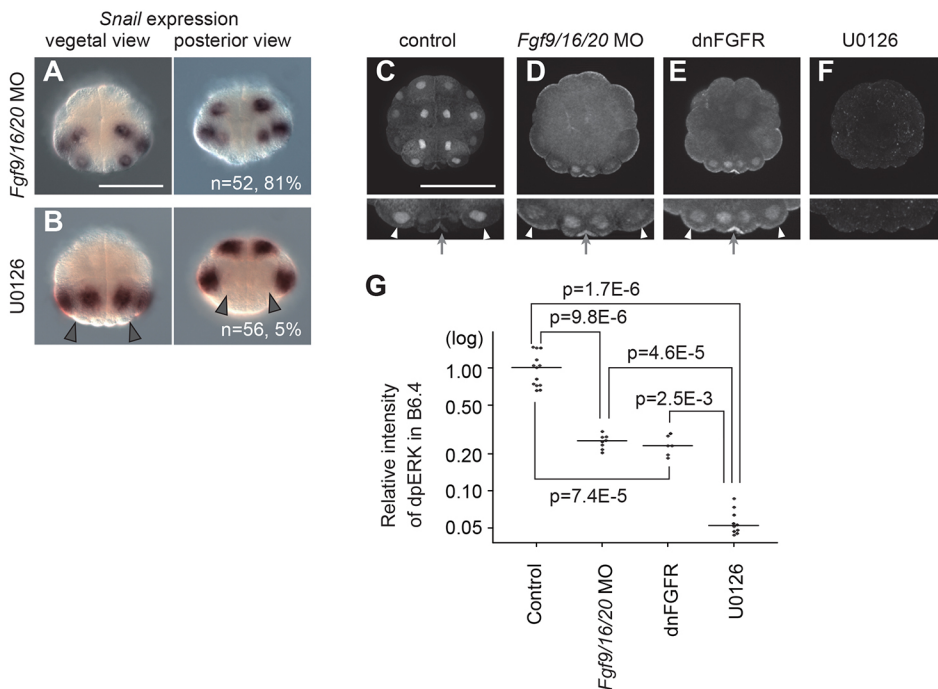
Fig. 4. The MAPK pathway is required for *Snail* expression in B6.4. (A,B) *Snail* expression in (A) *Fgf9/16/20* morphant and (B) U0126 (MEK inhibitor)-treated embryos. Gray arrowheads in (B) indicate the loss of *Snail* expression in B6.4 cells. The number of embryos examined and the proportion of embryos that clearly expressed *Snail* in B6.4 cells are shown within the panels. (C-F) Immunostaining with the antibody against dpERK of (C) control, (D) *Fgf9/16/20* morphant, (E) dnFGFR mRNA-injected and (F) U0126-treated embryos. Higher magnification views for posterior blastomeres (B6.3 and B6.4) are shown below. In the most posterior cells (B6.3), the dpERK signal is observed in nuclei and at the posterior pole (arrows) in (C-E). Arrowheads in (C-E) indicate B6.4 cells. Photographs are Z-projected image stacks. (G) Quantification of fluorescent intensity in the nuclei of B6.4 cells. The intensity was measured relative to the DAPI signal. The *y*-axis indicates the relative intensity for the average of the control on a log scale. Medians are indicated by black bars. Differences in relative intensity were analyzed by Wilcoxon rank-sum tests. Scale bars: 100 μm.

any partial embryos derived from *Raf* morphants (*n*=11 for the first *Raf* MO, and *n*=12 for the second MO) (Fig. 5G). Thus, it is likely that B6.3 and B6.4 activate the MAPK pathway to express *Snail* in the absence of a cell–cell interaction, and that *Raf* functions in this cell-autonomous pathway.

A splicing variant of *Raf* encodes a constitutively active form of the protein

A gene model for *Raf* indicated the possibility of two different transcript isoforms, both of which are supported by multiple expressed sequence tags (Satou et al., 2005, 2008) (Fig. 6A). Whereas the protein encoded by the first 'full' isoform contained three domains (CR1, CR2 and CR3) conserved widely from insects to vertebrates (Daum et al., 1994), the second 'ΔEx9' isoform was produced by skipping the ninth exon and the encoded protein lacked the second conserved domain (CR2) (Fig. 6B). Reverse transcription followed by PCR (RT-PCR) revealed that these two isoforms were present in fertilized eggs and 32-cell embryos (Fig. 6C).

The CR2 domain contains inhibitory phosphorylation sites, and mutant proteins with deletions, insertions or mutations of CR2 show high transforming activity (Chan et al., 2002; Chow et al., 1995; Heidecker et al., 1990; Ishikawa et al., 1988). Therefore, we tested the hypothesis that the ΔEx9 isoform acts as a constitutively active form in the ascidian embryo. For this purpose, we injected *Raf* mRNA together with the *Fgf9/16/20* MO into unfertilized eggs, and used anti-dpERK antibodies to examine the activity of the MAPK pathway at the 32-cell stage. As seen in embryos injected with the *Fgf9/16/20* MO alone (Fig. 4D), dpERK signals were detected only in B6.3 and B6.4 in most of the embryos co-injected with the *Fgf9/16/20* MO and the full isoform of *Raf* mRNA (Fig. 6D). By contrast, cells with a dpERK signal were markedly increased in embryos co-injected with the *Fgf9/16/20* MO and the ΔEx9 isoform of *Raf* mRNA (Fig. 6E). Indeed, the number of nuclei with a dpERK signal was significantly higher in the latter embryos than in the former embryos and in embryos injected with *Fgf9/16/20* MO only (Fig. 6H). Cells with a dpERK signal were also increased by

injection of the ΔEx9 isoform of *Raf* mRNA alone compared with uninjected control embryos (Fig. 6F,H). Thus, the ΔEx9 isoform acted as a constitutively active form.

Meanwhile, dpERK signals were lost in embryos that were injected with the ΔEx9 isoform of *Raf* mRNA and treated with U0126, which is a specific inhibitor of MEK (Fig. 6G,H). This observation suggested that the ΔEx9 isoform of *Raf* mRNA activated ERK through MEK, and further supported the conclusion that the ΔEx9 isoform acted as a constitutively active form.

Next, we injected mRNA encoding a fusion protein of Raf and a 3xFLAG tag into embryos. As a control, we also injected mRNA encoding a fusion protein of *lacZ* and a 3xFLAG tag. Immunostaining of these embryos with an anti-FLAG antibody showed that the Raf–3xFLAG fusion protein, but not the *lacZ*–3xFLAG fusion protein, was concentrated at the posterior pole (Fig. 6I,J). Therefore, it is possible that endogenous Raf protein is also concentrated at the posterior pole.

These results showed that *Snail* is activated by the combinatorial action of the MAPK pathway and Zic-r.a in the B6.4 lineage. At the same time, they raised the question why *Snail* is not activated in B5.1 at the 16-cell stage despite the fact that Zic-r.a functions as early as the 16-cell stage to turn on *Tbx6.b*, *Admp* and *Wnttun5* in B5.1 (Oda-Ishii et al., 2016), and that ΔEx9 *Raf* is expressed in fertilized eggs (Fig. 6C). To address this question, we quantified the signaling levels of dpERK in 16-cell embryos, and found that levels in B5.1 cells of 16-cell embryos were ~20% of those in B6.4 cells of 32-cell embryos (Fig. 7A,B). Therefore, it is likely that the MAPK pathway activity is not sufficiently strong in B5.1 at the 16-cell stage to activate *Snail*. Indeed, bFGF treatment induced *Snail* expression in B5.1 of 16-cell embryos, whereas control bovine serum albumin (BSA) treatment did not (Fig. 7C,D).

The nuclear dpERK signal level was found to be stronger in B5.2 than in the other vegetal blastomeres of 16-cell embryos (B5.1, A5.1, and A5.2) (Fig. 7A,B). This observation provides further support for the hypothesis that the MAPK pathway is activated cell-autonomously in the posterior cells.
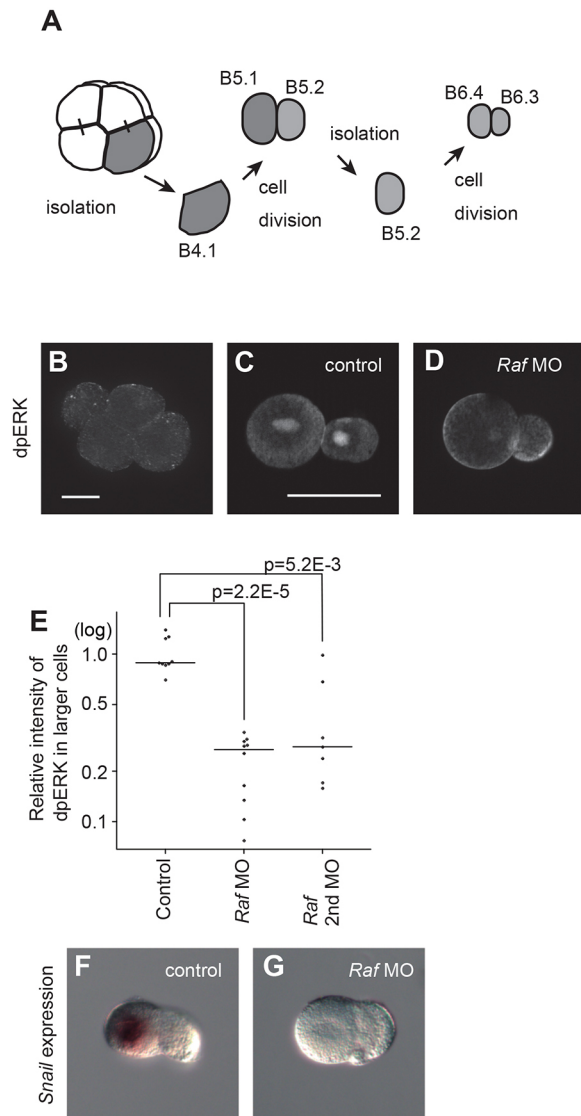
Fig. 5. The MAPK pathway is activated autonomously in the B6.4 lineage.
(A) Autonomous activation of the MAPK pathway was examined by isolating the posterior vegetal cells using a glass needle. At the 8-cell stage, the posterior vegetal cell, B4.1, was isolated. After the next division, a smaller cell was again isolated, and the resultant partial embryos were collected after the next division. (B) Immunostaining with the antibody against dpERK of an 8-cell embryo (*n*=57). (C,D) Immunostaining with the antibody against dpERK of partial embryos obtained from (C) control and (D) *Raf* morphants embryos. (E) Quantification of fluorescent intensity in the nuclei of larger cells. The intensity was measured relative to the DAPI signal. The *y*-axis indicates the relative intensity values for the average of the control on a log scale. Medians are shown by black bars. Differences in relative intensity against the controls were analyzed by Wilcoxon rank-sum tests. (F,G) *In situ* hybridization for *Snail* mRNA in partial embryos obtained from (F) control (*n*=7) and (G) *Raf* morphants embryos (*n*=11 for the first *Raf* MO, and *n*=12 for the second MO). Cells with *Snail* expression in (F) are likely to correspond to B6.4, given their size. Scale bars: 50 μm.

DISCUSSION
Two distinct mechanisms for activating *Snail* expression
Our study showed that *Snail* is activated by two distinct mechanisms in early *Ciona* embryos. In the B5.1 lineage, *Snail* is activated by Tbx6.b. This regulation is likely to be direct, because Tbx6.b is bound to the upstream sequence of *Snail* in early embryos (Kubo et al., 2010). Given that *Tbx6.b* is activated by the combinatorial action of

two maternal factors, β-catenin and Zic-r.a, in B5.1 at the 16-cell stage (Oda-Ishii et al., 2016), Zic-r.a might indirectly regulate *Snail* expression through *Tbx6.b* in this lineage. By contrast, in the B6.4 lineage, *Tbx6.b* is not expressed before *Snail* expression, and is unnecessary for the activation of *Snail*. Instead, Zic-r.a and MAPK pathway activation are required. Given that *Snail* expression in the B6.4 lineage begins immediately after the release from transcriptional repression, it is likely that Zic-r.a directly activates *Snail*. These two distinct (Tbx6.b-dependent and MAPK pathway-dependent) mechanisms cause the simultaneous expression of *Snail* at the 32-cell stage in the B5.1 and B6.4 cell lineages (Fig. 7E).

It is possible that the MAPK pathway-dependent mechanism functions in the B5.1 lineage of 32-cell embryos, because the MAPK pathway is activated in this lineage at the 32-cell stage (Fig. 4C). However, cells of the B5.1 lineage (B6.1 and B6.2) are expected to contain Zic-r.a less abundantly than B6.4 cells, because B6.4 cells and B6.1/B6.2 cells are daughter and granddaughter cells, respectively, of the most posterior cells, in which *Zic-r.a* mRNA is localized. For this reason, the Tbx6.b-dependent mechanism likely has the major role in activating *Snail* in the B5.1 lineage.

Similarly, B5.1 cells of 16-cell embryos might contain Zic-r.a less abundantly compared with B6.4 cells of 32-cell embryos, because Zic-r.a is produced from the mRNA localized at the posterior pole. Therefore, this might be another reason why the MAPK pathway-dependent mechanism does not function at the 16-cell stage, in addition to the insufficient level of dpERK in B5.1 cells of 16-cell embryos shown in Fig. 7B.

The most posterior cells contribute to germ cells, and transcription in these cells is repressed by Pem-1 (Kumano et al., 2011; Shirae-Kurabayashi et al., 2011). Given that Zic-r.a and Pem-1 are both localized at the posterior pole, Zic-r.a cannot activate its target before Pem-1 disappears. This is the likely reason why *Tbx6.b* is not activated in B5.2 (a parental cell of B6.4) at the 16-cell stage; therefore, the *Tbx6.b*-dependent mechanism cannot activate *Snail* in B6.4 at the 32-cell stage.

Cell-autonomous activation of the MAPK pathway
In normal development, the Fgf9/16/20 signal contributes to activation of the MAPK pathway in the posterior vegetal cells (B6.3 and B6.4), as shown by the observation that the dpERK signal level in *Fgf9/16/20* morphant embryos was reduced to 25% of that in unperturbed embryos (Fig. 4G). However, the MAPK pathway was activated even without this signal. Within the most posterior cells (B6.3), the dpERK signal was detected in nuclei and at the posterior pole, where many maternal mRNAs are localized (Matsuoka et al., 2013; Nishida and Sawada, 2001; Sasakura et al., 1998a,b; Satou, 1999; Satou and Satoh, 1997; Yamada, 2006; Yoshida et al., 1996). Therefore, it is conceivable that the MAPK pathway is activated by proteins derived from mRNAs localized at the posterior pole. This idea is consistent with the observation that activation of the MAPK pathway in B6.3 and B6.4 does not require signaling molecules from neighboring cells. Further support comes from the observation that the dpERK signal was observed in nuclei and at the posterior pole of the most posterior cells of the 16-cell embryo (Fig. 7A).

A constitutively active form of Raf
Our data strongly suggest that the constitutively active form of Raf (ΔEx9) is responsible for activation of the MAPK pathway at the posterior pole. First, the mRNA encoding the constitutively active form of Raf was present in both fertilized eggs and 32-cell embryos. Second, Raf activity was required for *Snail* expression in B6.4. Third, it is likely that Raf is concentrated at the posterior pole of
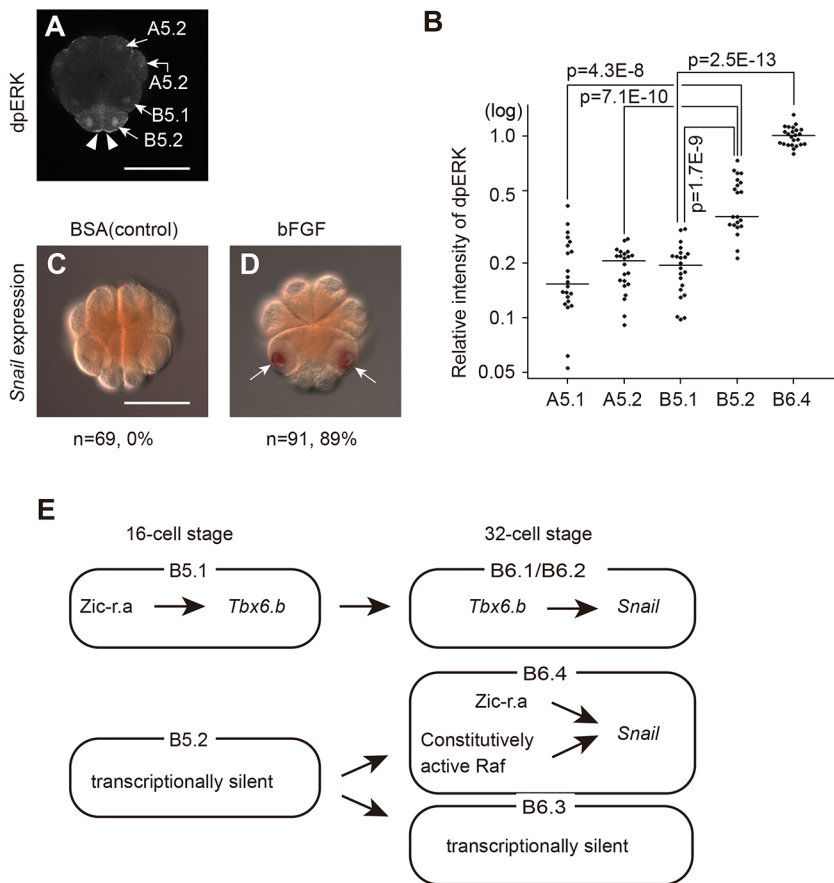
Fig. 6. A constitutively active form of Raf contributes to activation of the MAPK pathway in the posterior lineage.
(A) Genomic region encoding *Raf*. Two gene models, each of which is supported by ESTs, are predicted (Satou et al., 2008). (B) An alignment of the amino acid sequences encoded by the ninth exon of *Ciona Raf* with the corresponding sequence of human CRAF. The conserved region 2 (CR2) of CRAF is enclosed by a box, and conserved amino acids between human and *Ciona* proteins are shown by asterisks. (C) Two alternative splicing isoforms are confirmed by RT-PCR, which was performed with RNAs extracted from fertilized eggs and 32-cell embryos. Locations of primers used for PCR are shown by arrows on the left. (D-G) Immunostaining with an antibody against dpERK. Embryos injected with (D) *Raf* mRNA, (E) ΔEx9 *Raf* mRNA together with the *Fgf9/16/20* MO, and (F) ΔEx9 *Raf* mRNA alone, and (G) embryos that were injected with ΔEx9 *Raf* mRNA and treated with U0126 are shown. Photographs are Z-projected image stacks. Contrast and brightness of all images were linearly adjusted. (H) The number of nuclei stained with the antibody against dpERK was counted for controls and embryos injected with the *Fgf9/16/20* MO alone or in combination with the full or ΔEx9 *Raf* mRNA. Black bars indicate medians. Wilcoxon rank-sum tests were performed among embryos injected with the *Fgf9/16/20* MO and among embryos injected with ΔEx9 *Raf* mRNA and/or treated with U0126. (I,J) Immunostaining of embryos injected with mRNAs encoding proteins of (I) *lacZ* and (J) Raf with a 3xFLAG tag (*n*=40 for I and *n*=33 for J). An anti-FLAG antibody was used in the experiment. Only the Raf protein is observed at the posterior pole (arrowheads). Higher magnification views of the posterior pole are shown in I′ and J′. In I″ and J″, contrast and brightness were linearly adjusted for clarification. Scale bar: 100 μm.

early embryos, because the Raf–3xFLAG protein translated from the injected mRNA was concentrated at the posterior pole of 32-cell embryos. However, our data could not discriminate between whether the injected mRNA was localized at the posterior pole and thereby its product was observed there, or whether only the protein product was concentrated at the posterior pole. We favor the former hypothesis, because endogenous *Raf* mRNA is weakly localized at the posterior pole of early embryos (Imai et al., 2004; Yamada, 2006). Full and ΔEx9 isoforms of Raf might be translated

from mRNA localized in the most posterior cells with a germ cell fate, and the ΔEx9 isoform diffused from the posterior pole might activate the MAPK pathway in the most posterior cells (B5.2 of 16-cell embryos and B6.3 of 32-cell embryos) and their daughter cells (B6.4 of 32-cell embryos). Indeed, the nuclear dpERK signal level was stronger in B5.2 than in the other vegetal blastomeres of 16-cell embryos (B5.1, A5.1, and A5.2) (Fig. 7A,B). This observation supports the former hypothesis that the injected mRNA was localized in the posterior pole.

Fig. 7. The MAPK pathway is weakly activated in the posterior cells of 16-cell embryos. (A) Immunostaining with an antibody against dpERK in a 16-cell embryo. Arrowheads indicate the signal for the posterior pole. (B) Quantification of fluorescent intensity in the nuclei of four vegetal cells of 16-cell embryos and of B6.4 of 32-cell embryos. The average intensity was calculated relative to the DAPI signal. The y-axis indicates the relative values for the average of the control on a log scale. Differences in relative intensity between B5.2 and other vegetal blastomeres of 16-cell embryos and between B5.1 and B6.4 were analyzed by Wilcoxon rank-sum tests. (C,D) Snail expression in 16-cell embryos incubated in sea water containing (C) BSA and (D) recombinant bFGF. Precocious expression of Snail in B5.1 in (D) is indicated by arrows. The number of embryos examined and the proportion of embryos that expressed Snail are shown below the panels. (E) Summary of regulation of Snail. Scale bars: 100 μm.

Mutant Raf proteins with deletions, insertions or mutations of CR2 have a high transforming activity (Chan et al., 2002; Chow et al., 1995; Heidecker et al., 1990; Ishikawa et al., 1988), although such alternations do not necessarily promote the phosphorylation of Raf targets *in vitro*. In the ascidian embryo, the ΔEx9 Raf isoform, which lacked CR2, behaved as a constitutively active protein, and increased the level of phosphorylation of ERK. It is well established that Raf activates MEK, which in turn activates ERK (Imajo et al., 2006). Indeed, MEK was required for activation of ERK by the ΔEx9 isoform of Raf in the ascidian embryo (Fig. 6G).

The ΔEx9 isoform was utilized for normal developmental in the ascidian embryo. It is likely that, because the constitutively active form of *Raf* mRNA was a minor population, its protein product does not activate the MAPK pathway as strongly as Fgf9/16/20. Thus, despite the constitutive activation of the MAPK pathway, *Ciona* embryos will be able to respond to the Fgf9/16/20 signal, which activates the MAPK pathway more strongly. The activated MAPK pathway then activates downstream genes in cells other than B6.3 and B6.4 at the 32-cell stage (Bertrand et al., 2003; Hudson et al., 2016; Imai et al., 2002a; Ohta and Satou, 2013; Ohta et al., 2015). Hence, the level of activation of the MAPK pathway by the constitutively active form of Raf will need to be kept low. This will also be important for preventing this isoform from transforming embryonic cells. Therefore, RNA processing of *Raf* transcripts might be controlled strictly in ascidian embryos.

A shortcut gene circuit for the B6.4 lineage to catch up with the B5.1 lineage

In the ascidian embryo, somatic cells are separated from cells with a germ cell fate at each cell division. Given that transcription is suppressed in the germ line, the zygotic genetic program begins at different stages; the B6.4 lineage initiates the zygotic genetic program one stage later than the B5.1 lineage, in which maternal factors activate *Tbx6.b* at the 16-cell stage and Tbx6.b activates *Snail* at the 32-cell stage. The constitutively active form of Raf enables Zic-r.a to take a shortcut to directly activate *Snail* in the B6.4 lineage; therefore, *Snail* begins to be expressed immediately after initiation of the zygotic genetic program at the 32-cell stage (Fig. 7E). As a result, in both the B5.1 and B6.4 lineages, two key transcription factor genes, *Tbx6.b* and *Snail*, are expressed by the 32-cell stage, and the genetic program proceeds concurrently and in a coordinated manner in these lineages; Tbx6.b activates the muscle gene circuit, and Snail represses the ectopic expression of regulatory genes, including *Myt1* and *Brachyury*. We propose that such shortcuts for gene circuits might be required for the coordination of cellular developmental programs in embryos in which somatic cells are produced progressively from cells with a germ cell fate. Such shortcuts might also be used for coordination among cells that become separated progressively from stem cells.

MATERIALS AND METHODS

Animals, whole-mount *in situ* hybridization, and gene identifiers

C. intestinalis (type A; also called *C. robusta*) adults were obtained from the National Bio-Resource Project for *Ciona* (Japan). cDNA clones were obtained from our EST clone collection (Satou et al., 2005). Whole-mount *in situ* hybridization was performed as described previously (Satou et al., 1995). Identifiers for genes examined in the present study are as follows: KH.C3.751 for *Snail*, KH.L18.20 for *Raf*, KH.S654.1–3 for *Tbx6.b*, KH.C1.727 for *Zic-r.a*, KH.C2.125 for *Fgf9/16/20*, KH.C14.307 for *Mrf*, and KH.C1.274 for *Myt1*.

Gene knockdown, overexpression and reporter assays

Sequences of *Raf* MOs were 5′-CATTGTGGCCATCATTCTTTGCCAT-3′ and 5′-AATCTCCTAACTGATCTTCCAGTCA-3′, and sequences of *Snail* and *Fgf9/16/20* MOs were 5′-GTCATGATGTAATCACAGTAATATA-3′ and 5′-CATAGACATTTTCAGTATGGAAGGC-3′. *Snail* and *Fgf9/16/20* MOs have been used previously (Imai et al., 2006, 2009). Given that *Tbx6.b* is a multicopy gene, we injected a mixture of the following two MOs so that all copies were knocked down, as reported previously (Yagi et al., 2005): 5′-TTGAGCCTCTCACGTCTGTCGCCAT-3′ and 5′-TTACAATTTCCTC-TCTCTTTCGATT-3′. MOs were injected by microinjection under a microscope, as described previously (Satou et al., 2001a).

For *Raf* mRNA injection, the entire coding sequence and coding sequence lacking the ninth exon of *Raf* were cloned into pBluscript RN3 (Lemaire et al., 1995). mRNAs encoding Raf–3xFLAG and the *lacZ*–3xFLAG tag contain the 5′ and 3′ untranslated regions of *Raf*. These mRNAs were transcribed using the mMESSAGE mMACHINE T3 Transcription Kit (Thermo Fisher Scientific).

We performed all gene knockdown and/or overexpression experiments at least twice with different batches of embryos.

RNA sequencing

For RNA-seq experiments, we prepared normal control embryos and embryos injected with the *Snail* MO. At the 8-cell stage, we isolated the posterior vegetal cell pair (B4.1) with a fine glass needle. The isolated cells were incubated until unperturbed embryos reached the tailbud stage. RNA was extracted using a Dynabeads mRNA DIRECT Micro Kit (Thermo Fisher Scientific) and libraries were made with an Ion Total RNA-Seq kit v2 (Thermo Fisher Scientific). The libraries were sequenced with an Ion PGM instrument (Thermo Fisher Scientific). We performed the same experiment twice (biological duplicates). NOISeq (Tarazona et al., 2011) was used to identify differentially expressed genes.

Immunostaining and quantification of fluorescent intensity

Immunostaining with the anti-dpERK antibody (Sigma, M9692) and anti-FLAG antibody (Sigma, F1840) was performed as described previously (Ohta and Satou, 2013). ImageJ was used to quantify the fluorescent intensity. All photographs for comparisons were taken under the same conditions, and the DAPI signal intensity was used as a reference.

Reverse transcription followed by PCR

To quantify gene expression, we used the Cells-to-Ct kit (Thermo-Fisher Scientific). For each reaction, 15 embryos were lysed. Each specimen was divided into two fractions; reverse transcriptase (RT) was added to one fraction, and water was added into the other fraction as an RT(–) control. No amplification was observed in the RT(–) controls. Given that *Pou2* is maternally expressed and its expression is thought to remain constant in early embryos, we used it as an internal control. TaqMan chemistry was used in quantitative PCR, and the probes and primers are listed in Table S2.

To detect splicing variants of *Raf*, RNA was extracted using the RNeasy kit (Qiagen). After DNase treatment, each specimen was reverse transcribed with SuperScript II RT (Thermo Fisher Scientific), and then amplified with PCR using the following primers: 5′-GAAGAAAATCCGTCCCCAAAC-3′ and 5′-GTGGGCGGGCGGATAA-3′. No amplification was observed in control samples that included water instead of RT.

Author contributions

Conceptualization: M.T., Y.S.; Validation: M.T., Y.S.; Formal analysis: M.T., K.K., Y.S.; Investigation: M.T., K.K.; Writing - review and editing: M.T., K.K., Y.S.; Visualization: M.T.; Supervision: Y.S.; Project administration: Y.S.; Funding acquisition: Y.S.

Data availability

The RNA-seq data produced in the present study are available in the SRA database under the accession number SRP130046.

Supplementary information

Supplementary information available online at
http://dev.biologists.org/lookup/doi/10.1242/dev.163915.supplemental

References

Bertrand, V., Hudson, C., Caillol, D., Popovici, C. and Lemaire, P. (2003). Neural tissue in ascidian embryos is induced by FGF9/16/20, acting via a combination of maternal GATA and Ets transcription factors. *Cell* **115**, 615-627.

Chan, E. Y. W., Stang, S. L., Bottorff, D. A. and Stone, J. C. (2002). Mutations in conserved regions 1, 2, and 3 of Raf-1 that activate transforming activity. *Mol. Carcinogen.* **33**, 189-197.

Chow, Y.-H., Pumiglia, K., Jun, T. H., Dent, P., Sturgill, T. W. and Jove, R. (1995). Functional mapping of the N-terminal regulatory domain in the human Raf-1 protein-kinase. *J. Biol. Chem.* **270**, 14100-14106.

Daum, G., Eisenmanntappe, I., Fries, H.-W., Troppmair, J. and Rapp, U. R. (1994). The ins and outs of Raf kinases. *Trends Biochem. Sci.* **19**, 474-480.

Davidson, B., Shi, W., Beh, J., Christiaen, L. and Levine, M. (2006). FGF signaling delineates the cardiac progenitor field in the simple chordate, *Ciona intestinalis*. *Genes Dev.* **20**, 2728-2738.

Deno, T., Nishida, H. and Satoh, N. (1984). Autonomous muscle cell differentiation in partial ascidian embryos according to the newly verified cell lineages. *Dev. Biol.* **104**, 322-328.

Erives, A., Corbo, J. C. and Levine, M. (1998). Lineage-specific regulation of the *Ciona snail* gene in the embryonic mesoderm and neuroectoderm. *Dev. Biol.* **194**, 213-225.

Fujiwara, S., Corbo, J. C. and Levine, M. (1998). The snail repressor establishes a muscle/notochord boundary in the *Ciona* embryo. *Development* **125**, 2511-2520.

Haupaix, N., Stolfi, A., Sirour, C., Picco, V., Levine, M., Christiaen, L. and Yasuo, H. (2013). p120RasGAP mediates ephrin/Eph-dependent attenuation of FGF/ERK signals during cell fate specification in ascidian embryos. *Development* **140**, 4347-4352.

Heidecker, G., Huleihel, M., Cleveland, J. L., Kolch, W., Beck, T. W., Lloyd, P., Pawson, T. and Rapp, U. R. (1990). Mutational activation of C-Raf-1 and definition of the minimal transforming sequence. *Mol. Cell. Biol.* **10**, 2503-2512.

Hibino, T., Nishikata, T. and Nishida, H. (1998). Centrosome-attracting body: a novel structure closely related to unequal cleavages in the ascidian embryo. *Dev. Growth Differ.* **40**, 85-95.

Hudson, C., Lotito, S. and Yasuo, H. (2007). Sequential and combinatorial inputs from Nodal, Delta2/Notch and FGF/MEK/ERK signalling pathways establish a grid-like organisation of distinct cell identities in the ascidian neural plate. *Development* **134**, 3527-3537.

Hudson, C., Sirour, C. and Yasuo, H. (2016). Co-expression of Foxa.a, Foxd and Fgf9/16/20 defines a transient mesendoderm regulatory state in ascidian embryos. *Elife* **5**, e14692.

Ikeda, T. and Satou, Y. (2017). Differential temporal control of *Foxa.a* and *Zic-r.b* specifies brain versus notochord fate in the ascidian embryo. *Development* **144**, 38-43.

Ikeda, T., Matsuoka, T. and Satou, Y. (2013). A time delay gene circuit is required for palp formation in the ascidian embryo. *Development* **140**, 4703-4708.

Imai, K., Satoh, N. and Satou, Y. (2002a). Early embryonic expression of *FGF4/6/9* gene and its role in the induction of mesenchyme and notochord in *Ciona savignyi* embryos. *Development* **129**, 1729-1738.

Imai, K. S., Satou, Y. and Satoh, N. (2002b). Multiple functions of a Zic-like gene in the differentiation of notochord, central nervous system and muscle in *Ciona savignyi* embryos. *Development* **129**, 2723-2732.

Imai, K. S., Hino, K., Yagi, K., Satoh, N. and Satou, Y. (2004). Gene expression profiles of transcription factors and signaling molecules in the ascidian embryo: towards a comprehensive understanding of gene networks. *Development* **131**, 4047-4058.

Imai, K. S., Levine, M., Satoh, N. and Satou, Y. (2006). Regulatory blueprint for a chordate embryo. *Science* **312**, 1183-1187.

Imai, K. S., Stolfi, A., Levine, M. and Satou, Y. (2009). Gene regulatory networks underlying the compartmentalization of the *Ciona* central nervous system. *Development* **136**, 285-293.

Imajo, M., Tsuchiya, Y. and Nishida, E. (2006). Regulatory mechanisms and functions of MAP kinase signaling pathways. *IUBMB Life* **58**, 312-317.

Ishikawa, F., Sakai, R., Ochiai, M., Takaku, F., Sugimura, T. and Nagao, M. (1988). Identification of a transforming activity suppressing sequence in the C-Raf oncogene. *Oncogene* **3**, 653-658.

DEVELOPMENT

Kobayashi, K., Sawada, K., Yamamoto, H., Wada, S., Saiga, H. and Nishida, H. (2003). Maternal macho-1 is an intrinsic factor that makes cell response to the same FGF signal differ between mesenchyme and notochord induction in ascidian embryos. *Development* **130**, 5179-5190.

Kubo, A., Suzuki, N., Yuan, X., Nakai, K., Satoh, N., Imai, K. S. and Satou, Y. (2010). Genomic cis-regulatory networks in the early *Ciona intestinalis* embryo. *Development* **137**, 1613-1623.

Kumano, G., Takatori, N., Negishi, T., Takada, T. and Nishida, H. (2011). A maternal factor unique to ascidians silences the germline via binding to P-TEFb and RNAP II regulation. *Curr. Biol.* **21**, 1308-1313.

Lemaire, P., Garrett, N. and Gurdon, J. B. (1995). Expression cloning of Siamois, a *Xenopus* homeobox gene expressed in dorsal-vegetal cells of blastulae and able to induce a complete secondary axis. *Cell* **81**, 85-94.

Matsuoka, T., Ikeda, T., Fujimaki, K. and Satou, Y. (2013). Transcriptome dynamics in early embryos of the ascidian, *Ciona intestinalis*. *Dev. Biol.* **384**, 375-385.

Miwata, K., Chiba, T., Horii, R., Yamada, L., Kubo, A., Miyamura, D., Satoh, N. and Satou, Y. (2006). Systematic analysis of embryonic expression profiles of zinc finger genes in *Ciona intestinalis*. *Dev. Biol.* **292**, 546-554.

Nishida, H. and Sawada, K. (2001). macho-1 encodes a localized mRNA in ascidian eggs that specifies muscle fate during embryogenesis. *Nature* **409**, 724-729.

Oda-Ishii, I., Kubo, A., Kari, W., Suzuki, N., Rothbächer, U. and Satou, Y. (2016). A maternal system initiating the zygotic developmental program through combinatorial repression in the ascidian embryo. *PLoS Genet.* **12**, e1006045.

Ohta, N. and Satou, Y. (2013). Multiple signaling pathways coordinate to induce a threshold response in a chordate embryo. *PLoS Genet.* **9**, e1003818.

Ohta, N., Waki, K., Mochizuki, A. and Satou, Y. (2015). A boolean function for neural induction reveals a critical role of direct intercellular interactions in patterning the ectoderm of the ascidian embryo. *PLoS Comput. Biol.* **11**, e1004687.

Picco, V., Hudson, C. and Yasuo, H. (2007). Ephrin-Eph signalling drives the asymmetric division of notochord/neural precursors in *Ciona* embryos. *Development* **134**, 1491-1497.

Robert, V. J., Garvis, S. and Palladino, F. (2015). Repression of somatic cell fate in the germline. *Cell. Mol. Life Sci.* **72**, 3599-3620.

Sasakura, Y., Ogasawara, M. and Makabe, K. W. (1998a). *HrWnt-5*: a maternally expressed ascidian Wnt gene with posterior localization in early embryos. *Int. J. Dev. Biol.* **42**, 573-579.

Sasakura, Y., Ogasawara, M. and Makabe, K. W. (1998b). Maternally localized RNA encoding a serine/threonine protein kinase in the ascidian, Halocynthia roretzi. *Mech. Dev.* **76**, 161-163.

Satou, Y. (1999). *posterior end mark 3* (*pem-3*), an ascidian maternally expressed gene with localized mRNA encodes a protein with *Caenorhabditis elegans* MEX-3-like KH domains. *Dev. Biol.* **212**, 337-350.

Satou, Y. and Satoh, N. (1997). *posterior end mark 2* (*pem-2*), *pem-4*, *pem-5*, and *pem-6*: Maternal genes with localized mRNA in the ascidian embryo. *Dev. Biol.* **192**, 467-481.

Satou, Y., Kusakabe, T., Araki, S. and Satoh, N. (1995). Timing of initiation of muscle-specific gene-expression in the ascidian embryo precedes that of developmental fate restriction in lineage cells. *Dev. Growth Differ.* **37**, 319-327.

Satou, Y., Imai, K. and Satoh, N. (2001a). Action of morpholinos in Ciona embryos. *Genesis* **30**, 103-106.

Satou, Y., Takatori, N., Yamada, L., Mochizuki, Y., Hamaguchi, M., Ishikawa, H., Chiba, S., Imai, K., Kano, S., Murakami, S. D. et al. (2001b). Gene expression profiles in *Ciona intestinalis* tailbud embryos. *Development* **128**, 2893-2904.

Satou, Y., Yagi, K., Imai, K. S., Yamada, L., Nishida, H. and Satoh, N. (2002). *macho-1*-Related genes in *Ciona* embryos. *Dev. Genes Evol.* **212**, 87-92.

Satou, Y., Kawashima, T., Shoguchi, E., Nakayama, A. and Satoh, N. (2005). An integrated database of the ascidian, *Ciona intestinalis*: towards functional genomics. *Zool. Sci.* **22**, 837-843.

Satou, Y., Mineta, K., Ogasawara, M., Sasakura, Y., Shoguchi, E., Ueno, K., Yamada, L., Matsumoto, J., Wasserscheid, J., Dewar, K. et al. (2008). Improved genome assembly and evidence-based global gene model set for the chordate *Ciona intestinalis*: new insight into intron and operon populations. *Genome Biol.* **9**, R152.

Shirae-Kurabayashi, M., Matsuda, K. and Nakamura, A. (2011). Ci-Pem-1 localizes to the nucleus and represses somatic gene transcription in the germline of *Ciona* intestinalis embryos. *Development* **138**, 2871-2881.

Strome, S. and Lehmann, R. (2007). Germ versus soma decisions: Lessons from flies and worms. *Science* **316**, 392-393.

Tarazona, S., Garcia-Alcalde, F., Dopazo, J., Ferrer, A. and Conesa, A. (2011). Differential expression in RNA-seq: a matter of depth. *Genome Res.* **21**, 2213-2223.

Yagi, K., Satoh, N. and Satou, Y. (2004). Identification of downstream genes of the ascidian muscle determinant gene Ci-macho1. *Dev. Biol.* **274**, 478-489.

Yagi, K., Takatori, N., Satou, Y. and Satoh, N. (2005). Ci-Tbx6b and Ci-Tbx6c are key mediators of the maternal effect gene *Ci-macho1* in muscle cell differentiation in *Ciona intestinalis* embryos. *Dev. Biol.* **282**, 535-549.

Yamada, L. (2006). Embryonic expression profiles and conserved localization mechanisms of pem/postplasmic mRNAs of two species of ascidian, *Ciona intestinalis* and *Ciona savignyi*. *Dev. Biol.* **296**, 524-536.

Yoshida, S., Marikawa, Y. and Satoh, N. (1996). Posterior end mark, a novel maternal gene encoding a localized factor in the ascidian embryo. *Development* **122**, 2005-2012.
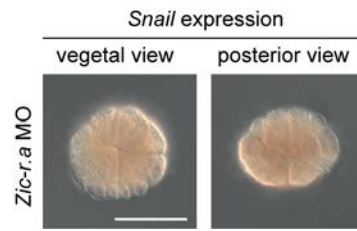
DEVELOPMENT

Figure S1. *Snail* is regulated by the maternal factor Zic-r.a. Whole-mount in situ hybridization for *Snail* mRNA in *Zic-r.a* morphant embryos. *Snail* expression was not observed in 29 of 30 embryos examined. Scale bar, 100 μm.

Table S1. Differentially expressed genes in *Snail* morphant partial embryos.

Gene	Fold of Change (morphant rpkm / control rpkm)	Expression
Upregulated genes in *Snail* morphants		
KH.C4.146	NA (7.74/0)	epidermis
Myt1 (KH.C1.274)	48.93 (15.69/0.32)	nervous system, mesenchyme
Epi1 (KH.C1.188)	42.51 (41.66/0.98)	epidermis
KH.C7.455	25.78 (46.92/1.82)	nervous system
KH.C8.510	19.17 (4.62/0.24)	epidermis
Pitx (KH.L153.79)	13.86 (5.19/0.37)	nervous system
Hes.a (KH.C1.159)	7.94 (49.22/6.19)	muscle, epidermis
KH.S164.13	7.73 (61.28/7.92)	notochord, epidermis, endoderm, nervous system
Snail (KH.C3.751)	5.11 (326.31/63.87)	muscle
KH.S1012.1	3.82 (613.13/160.3)	endoderm
KH.C9.203	2.94 (57.86/19.67)	nervous system
Chd (*chordin*; KH.C6.145)	2.9 (74.35/25.65)	nervous system
sFRP1/5 (KH.L171.5)	2.54 (145.72/57.45)	endoderm, epidermis
Zf266 (KH.C1.777)	2.33 (90.7/38.86)	mesenchyme, notochord, nervous system
Crebzf.a (KH.L108.4)	2.22 (162.52/73.17)	epidermis
KH.C11.697	2 (116.12/57.96)	notochord, endoderm, brain, nervous system
Downregulated genes in *Snail* morphants		
Isl (KH.L152.2)	0 (0/3.3)	nervous system
Tbx15/18/22 (*VegTR*) (KH.S589.4)	0.06 (0.97/16.24)	muscle
KH.L84.14	0.06 (2.6/42.3)	muscle
KH.S455.4	0.13 (3.88/30.72)	muscle
Mrf (*MyoD*) (KH.C14.307)	0.16 (6.64/40.87)	muscle
muscle actin (KH.C1.570)	0.17 (693.63/4049.83)	muscle
KH.C4.231	0.17 (17.51/100.6)	muscle, epidermis
muscle actin (KH.C8.649)	0.17 (38.9/222.85)	muscle
muscle actin (KH.C1.242)	0.19 (670.66/3544.06)	muscle
Hlx (KH.C11.657)	0.2 (12.72/64.59)	mesenchyme
muscle actin (KH.C7.67)	0.22 (352.83/1610.95)	muscle
muscle actin (KH.C4.343)	0.24 (253.08/1067.45)	muscle
muscle creatine kinase (KH.L10.5)	0.24 (108.27/455.46)	muscle
myosin light chain (KH.C1.1186)	0.24 (317.58/1331.2)	muscle
muscle actin (KH.S1440.1)	0.25 (541.25/2159.43)	muscle
myosin regulatory light chain (KH.C8.477)	0.28 (543.33/1960.28)	muscle
KH.C7.476	0.28 (31.41/111.06)	muscle
tropomyosin (KH.C3.661)	0.3 (583.28/1965.44)	muscle

KH.L4.23	0.32 (247.99/765.52)	muscle
myosin regulatory light chain (KH.C8.309)	0.35 (476/1372.56)	muscle
KH.C11.121	0.37 (75.89/202.62)	muscle, epidermis, endoderm, nervous system, mesenchyme
KH.S770.1	0.39 (58.4/149.79)	epidermis, mesenchyme
myosin regulatory light chain (KH.C8.859)	0.41 (287.26/706.18)	muscle
KH.C14.291	0.45 (80.26/177.22)	mesenchyme
KH.L17.2	0.45 (163.43/360.11)	muscle, trunk ventral cells (adult heart precursors)
Zf306 (KH.C1.669)	0.47 (26.37/56.65)	muscle, mesenchyme, notochord, nervous system
KH.C14.330	0.48 (65.98/136.75)	epidermis

Table S2. Primers and probes for RT-qPCR.

Gene	Probes and Primers
Mrf	Probe : 5′-FAM-CCCTTAAGCGTTGCGCATGCG-TAMRA-3′
	Forward primer : 5′-CGTGTCAACCAAGCGTACGA-3′
	Reverse primer : 5′-GGAAGTCTCTGGTTCGGGTTT-3′
Pou2	Probe : 5′-VIC-TGGTCCAGCCAAATCACTCACGCCTA-TAMRA-3′
	Forward primer : 5′-TACCACAGCATACACTGGACAACA-3′
	Reverse primer : 5′-GGCGCTGAGGTAATGCTTTG-3′